Use of a Heated Graphite Scrubber as a Means of Reducing Interferences in UV-Absorbance Measurements of Atmospheric Ozone

Andrew A. Turnipseed, Peter C. Andersen, Craig J. Williford, Christine A. Ennis, and John W.

5   Birks

2B Technologies, Inc., 2100 Central Ave., Boulder, CO 80301
Correspondence to: Andrew Turnipseed (andrewt@twobtech.com)

Abstract:

10   A new solid-phase scrubber for use in conventional ozone photometers was investigated as a
means of reducing interferences from other UV-absorbing species and water vapor. It was found that
when heated to 100-130°C, a tubular graphite scrubber efficiently removed up to 500 ppb ozone and
ozone monitors using the heated graphite scrubber were found to be less susceptible to interferences from
water vapor, mercury vapor, and aromatic volatile organic hydrocarbons (VOCs) compared to

15   conventional metal oxide scrubbers. Ambient measurements from a graphite scrubber-equipped
photometer and a co-located Federal Equivalent Method (FEM) ozone analyzer showed excellent
agreement over 38 days of measurements and indicated no loss in the scrubber's ability to remove ozone
when operated at 130°C. The use of a heated graphite scrubber was found to reduce the interference from
mercury vapor to ≤ 3% of that obtained using a packed-bed Hopcalite scrubber. For a series of

20   substituted aromatic compounds (ranging in volatility and absorption cross section at 253.7 nm), the
graphite scrubber was observed to consistently exhibit reduced levels of interference, typically by factors
of 2.5 to 20 less than with Hopcalite. Conventional solid-phase scrubbers also exhibited complex VOC
adsorption and desorption characteristics that were dependent upon the relative humidity (RH), volatility
of the VOC, and the available surface area of the scrubber. This complex behavior involving humidity is

25   avoided by use of a heated graphite scrubber. These results suggest that heated graphite scrubbers could
be substituted in most ozone photometers as a means of reducing interferences from other UV-absorbing
species found in the atmosphere. This could be particularly important in ozone monitoring for
compliance with the U.S. Clean Air Act or for use in VOC-rich environments such as in smog chambers
and monitoring indoor air quality.

1 Introduction

Ozone (O_3) in the lower atmosphere is produced by a complex set of photochemical reactions involving oxides of nitrogen and volatile organic compounds (VOCs). It is well established that anthropogenic emissions of these precursors lead to the production of elevated levels of ozone (Haagen-Smit and Fox, 1954; Chameides and Walker, 1973). It also is recognized that high levels of ozone are deleterious to human health (White et al., 1994; Weisel et al., 1995; Burnett et al., 1997; U.S-EPA, 2016) and lead to plant and crop damage (Avnery et al., 2011; Emberson, 2003; Emberson et al., 2009). For these reasons, the Clean Air Act in the U.S. and similar laws in other countries have set limits on ozone concentrations in ambient air. Enforcement of compliance with the U.S. National Ambient Air Quality Standards (NAAQS) requires monitoring of ozone concentrations at hundreds of locations, especially during summer months when photochemical ozone production is highest.

Currently, compliance monitoring of ozone is done almost exclusively by the method of UV absorbance at 253.7 nm due to the simplicity and reliability of this technique. However, it has been shown that UV photometers suffer from positive interferences from other trace gases that absorb at 253.7 nm such as mercury (Hg) and VOCs (Huntzicker and Johnson, 1979; Grosjean and Harrison, 1985; Kleindienst et al., 1993; Spicer et al., 2010). In addition, water vapor, which does not absorb at 253.7 nm, is also a significant interference in commercial ozone analyzers (Meyer et al., 1991; Kleindienst et al., 1993) due to its ability to change the transmission of light through the absorbance cell (Wilson and Birks, 2006). Field observations have noted possible interferences in conventional UV-absorbance ozone monitors in very highly polluted areas, such as Houston, TX (Olllison et al., 2013) and Mexico City (Leston et al, 2005); however, other extensive studies have not shown evidence of biases, even near urban areas (Ryerson et al., 1999; Parrish and Fehsenfeld, 2000). Average concentrations of interfering species found in outdoor air would normally be expected to cause errors of only a few ppb at most, but this is well within measurement limits of UV ozone photometers when averaged over the one hour time frame typical for compliance monitoring. Since high levels of interferences often coincide with high levels of ambient outdoor ozone (Leston et al., 2005; Ollison et al., 2013), a small, unpredictable bias would be difficult to discern and could result in regions being in non-compliance with the EPA ozone standard. The recent downward revision of the standard from 75 to 70 ppb (8-hr average) is expected to increase the number of U.S. counties being out of compliance from 224 to 241 (McCarthy and Lattanzio, 2016), making small ppb-level interferences a more critical issue.

Other applications where interferences can play a significant role in biasing UV-absorption O_3 measurements includes chamber-type experiments and the monitoring of indoor ozone. In the former, high VOC concentrations are typically used to enhance photochemistry (e.g., Leston et al., 2005; Griffin et al., 1999) or to generate aerosols (e.g., Lee et al., 2006), thus requiring accurate O_3 concentrations to be

65 made in VOC-rich atmospheres. Indoor ozone concentrations are typically 20-80% of that measured

outdoors (U.S.-EPA, 2016); however, interfering species such as VOCs and mercury can be at much

higher concentrations indoors from attached garages, cooking emissions, unvented heaters, the use of

paints, cleaners, and outgassing from building components. This places even more stringent constraints

on ozone monitors to reduce biases in these indoor environments.

70   Ambient ozone UV-absorbance measurements are conducted by observing the attenuation of

transmission of the mercury emission line at 253.7 nm (near the maximum in the ozone absorption

spectrum) through an absorbance cell. Relative light intensities are measured for a direct air sample (I)

and an air sample where the ozone is removed by some type of ozone scrubber (I_o), and the ozone

concentration computed using the Beer-Lambert Law. Ozone scrubbers are typically composed of

75 manganese dioxide, charcoal, Hopcalite, metal oxide coated screens, or heated silver wool and play a key

role in the degree to which interferences compromise the ozone readings in UV absorption photometers.

For chemical species that absorb 253.7 nm light, the degree of interference depends on the compound's

absorption cross section, its ambient concentration, and the degree to which the compound is removed by

the scrubber. If not removed by the scrubber, its concentration remains constant between I and I_o

80 measurements and cancels out in the Beer-Lambert Law. Thus the ideal scrubber would have two

characteristics: (1) it would quantitatively remove ozone; and (2) it would *not* remove other species that

absorb at 253.7 nm or that otherwise modify light transmission to the detector such as water vapor. The

metal oxide scrubbers used in conventional commercially available ozone photometers do not fully meet

the second criterion, leading to errors in the Beer-Lambert Law calculation of ozone.

85   A further, less obvious problem with UV-absorbing species is that they can desorb from the solid-

phase scrubber at later times, causing a negative absorbance (value of I_o is less than I in ozone-free air),

thus imparting a negative bias to the overall measurement. . This desorption can be caused by

temperature or relative humidity changes within the scrubber that alter the adsorption characteristics of a

species and allows it to be released back into the gas phase. Because UV-absorbing compounds and

90 mercury are commonly present to some degree in both indoor and outdoor air, these interferences may be

responsible in part for the baseline drift that occurs in photometric ozone monitors (Birks et al., 2013;

Ollison et al., 2013). Therefore development of a solid phase scrubber that effectively destroys ozone ($\geq$

99% destruction), but efficiently passes interfering species is desirable.

Table 1 provides a list of several atmospheric constituents with known 253.7-nm absorption cross

95 sections along with a selectivity ratio (S), defined as the ratio of the ozone cross section to that of the

interfering compound at 253.7 nm. Notable among these are VOCs that contain an aromatic group. The

absorption cross sections of these compounds vary widely, but can be similar to that of ozone, depending

on the types of functional groups attached. Gaseous mercury is a particularly strong interference because

the electronic energy levels of Hg atoms are resonant with the Hg emission line used in most ozone
monitors. The relative response of mercury has been estimated at ~1 ppb O_3/ppt Hg (Spicer et al., 2010; Li et al., 2006). So even a few ppt of mercury vapor can potentially cause substantial biases in ozone measurements.

In this study we present a means of greatly reducing the interferences of mercury, UV-absorbing VOCs, and water vapor in ozone measurements by replacing conventional metal oxide internal ozone scrubbers with a heated graphite scrubber (Birks et al., 2016). Carbon-based scrubbers have often been used for removing ozone from air (Shields et al., 1999; Lee and Davidson, 1999). However, these scrubbers also effectively remove many other compounds (such as VOCs and water) by adsorption due to their large surface area (typically 500-3000 m^2/g) and thus provide no significant advantage over existing ozone scrubbers. On the other hand, carbon in the form of graphite has a more ordered planar structure with less surface area (often < 20 m^2/g) and fewer sites available for adsorption of possible interfering compounds. We show that a heated graphite scrubber composed of one or more graphite tubes effectively destroys ozone while efficiently passing most UV-absorbing species and is relatively insensitive to humidity changes. Our results suggest that replacement of conventional scrubbers in commercially available ozone photometers with heated graphite scrubbers could increase their accuracy by reducing potential interferences.

2   Experimental

Most experiments were carried out with modified FEM 2B Technologies, Model 202 Single-Beam and Dual-Beam Model 205 or Model 211 Ozone Monitors. Figure 1a shows a diagram of a typical single-beam UV ozone photometer such as the Model 202. Ambient air samples are drawn into the instrument through an inlet via an air pump. A solenoid valve alternately switches the gas sample directly into the optical detection cell or through an ozone scrubber and then into the detection cell. UV light from a low-pressure mercury lamp UV light passes through the detection cell and is detected by a photodiode containing a built-in interference filter centered at 254 nm. The ozone concentration is calculated using the Beer-Lambert Law,

$$[O_3] = \frac{1}{\sigma L} \ln\left(\frac{I_o}{I}\right) \tag{1}$$

where σ is the absorption cross section for ozone (1.15 x 10^{-17} cm^2 molecule^{-1}), L is the path of the detection cell, I_o is the lamp intensity at the detector in the absence of ozone, and I is the lamp intensity with ozone present. The path length (L) is 15 cm for the 2B Technologies Models 202 and 205 Ozone Monitors. The Model 205 (and Model 211) analyzer differs in that it is a typical dual-beam instrument

containing two optical cells irradiated by the same lamp, but with each cell equipped with its own photodiode.   Two 3-way solenoid valves are switched to alternate passage of ozone-scrubbed and un-scrubbed air through the two cells, providing a simultaneous measurement of I and I_o. These analyzers were modified to locate the ozone scrubber outside of the instrument, allowing for easy exchange between

135   the different scrubbers tested.   Mixtures of interfering compounds in air were sampled into the ozone analyzers via an overflow tee where excess air was vented through a second scrubber to the atmosphere. All analyzers used were operating at manufacturer specifications.

Graphite scrubbers consisted of different combinations of graphite tubes (¼-in o.d. and 1/8-in i.d., Ohio Carbon Blank, EDM-AF5 graphite) housed in a temperature-controlled aluminum block. Tube

140   lengths were either 7.6 cm (3-in) or 15.2 cm (6-in). Most results were obtained using four 3-in tubes plumbed in parallel as shown in Figure 1b. Using multiple tubes increased both surface area and residence time while still maintaining high flow conductance. This configuration was chosen because it quantitatively destroyed (>99%) ozone in the single-beam Model 202 Ozone Monitor and fit within both Model 202 and 205 instruments. The aluminum block was heated with a cartridge heater (Thermal Corp.,

145   #CPN20528), whose temperature could be varied up to 160°C and controlled to within ±2°C. The graphite tubes were cleaned before use by heating at 300°C for 12 hours while purging with UHP nitrogen and sonication for 20 min in dilute Micro-90 glass cleaner followed by rinsing with distilled water and drying. Scrubbers consisting of coarsely ground EDM-AF5 graphite (~ 1-3 mm diameter particles) were also tested and exhibited similar properties for both ozone destruction and the reduction of

150   interferences. However, we present results from the tube scrubbers because their geometric surface area and residence times were more easily characterized.

Other commercially available scrubbers were included in this study for comparison. These include the conventional packed-bed Hopcalite scrubber used in 2B Technologies analyzers, and manganese oxide-coated screens from a Thermo Electron Model 49c and a Teledyne-Advanced Pollution

155   Instrumentation Model 400E.   We also tested heated silver wool scrubbers similar to scrubbers used by Horiba. It should be noted that although these various scrubbers were used within 2B Technologies analyzers, pressure and flow conditions were similar to those in the respective commercial analyzers. However, small differences in operating conditions of the various commercial analyzers may alter results in those instruments compared to those presented here.

160   Dry air (< 2% relative humidity (RH)) was produced using a zero air generator (Aadco, Model 737) or from cylinders of zero grade air. Ozone/air mixtures and ozone-free air were produced via an ozone calibrator – a Model 306 Ozone Calibration Source™ (2B Technologies). The Model 306 instrument qualifies as an EPA transfer standard for ozone and can produce known mixing ratios of ozone via UV photolysis of air in the range 0 and 1 ppm. Humidity was varied by humidifying the source air for

165   the Model 306. A mixing tee was placed on the source line of the Model 306 with one end pulling

through a water bubbler and the other through a drying tube (Drierite). Needle valves on each line

allowed for independent control over the source line between the dry and humid air. Humidity was

measured in the overflow just downstream of the ozone monitor via a temperature/humidity sensor

(Omega, Model HH311).

170   Mercury vapor was introduced to the ozone analyzer by using a glass diffusion tube. A small

amount of liquid mercury was placed in a glass bulb and vapor was allowed to diffuse through a 20-cm

long capillary tube (i.d. = 0.5 mm). At the exit of the capillary tube, a small sweep flow of air (~ 5-15

cc/min) purged the mercury vapor into the main airflow (~ 3 Lpm). Mercury concentrations were varied

by immersing the reservoir and capillary tube in an insulated water bath and varying the temperature of

175   the bath (0 to 60°C). From bath temperature, flow rates and the mercury vapor pressure, estimated

mercury vapor concentrations of 0.3 to 30 ppb were produced. Mercury interference measurements were

made relative to the 2B packed-bed Hopcalite scrubber.

Table 1 summarizes the absorption cross sections at 253.7 nm for a variety of atmospheric species

including compounds tested in this study. Test compounds were chosen because they are either common

180   outdoor (p-xylene) or indoor (phenol) pollutants or for comparison with previous studies (Spicer et al.,

2010). Typically, gas mixtures between 5 and 25 ppm were made in pre-conditioned gas cylinders by

dilution of the pure compound in UHP nitrogen. These were further diluted with zero grade air via mass

flow controllers to produce mixing ratios in the range of 0.01-1.4 ppm. Low volatility (o-nitrophenol)

VOCs were added using diffusion tubes similar to that described for mercury above. Sample purity was

185   assessed using a gas chromatograph with flame ionization and mass spectrometric detection (GC-FID,-

MS). The VOC/air mixtures were sampled into ozone analyzers equipped with different scrubbers from

an overflow tee. In some experiments, the VOC/air flow was simultaneously sampled into the inlet

system of a gas chromatograph equipped with a flame ionization detector (GC-FID). VOC samples were

pre-concentrated via a cooled (-5°C) focusing trap containing Tenax-TA (typically 100-500 cm^3 of the

190   VOC/air mixture) and then rapidly heated to inject as described in Greenberg et al. (1994). Both GC

systems were calibrated with a NIST-certified primary standard of neohexane in nitrogen or a secondary

VOC standard containing isoprene and camphene.

3   Results and discussions

195   As mentioned previously, any species absorbing light at 253.7 nm will be detected if its

concentration is changed by the ozone scrubber, and thus an ideal ozone scrubber would remove all ozone

but quantitatively pass interferents such as water vapor and UV-absorbing species. The following

sections test the graphite scrubber against this ideal, followed by comparative tests with existing conventional scrubbers for known interferences.

3.1 Ozone removal efficiency

It has long been known that ozone reacts with graphite (Hennig, 1965; Tracz et al., 2003;), causing loss of the carbon surface (Razumovskii et al., 2007) with the assumed production of CO and CO_2. CO and CO_2 have been identified as the primary products from reactions of ozone with carbon black aerosols which are thought to be similar to graphitic carbon (Stephens et al., 1989; Smith and Chughtai, 1996; Saathoff et al., 1998). CO, CO_2, and other possible low volatility hydrocarbons which could be lost to the gas phase tend to show negligible absorption at 253.7 nm (Table 1) compared to ozone. A graphite scrubber is not catalytic (i.e., there is actual loss of the scrubber carbon), but it can be estimated that a typical 3-inch long graphite tube would require a continuous 200 ppb ozone exposure at a flow rate of 1 Lpm for 213 days to lose 1% of its carbon; at 100°C oxidation by ambient O_2 is also negligible (Entegris, 2015).

Initial tests of the graphite scrubber using four parallel 15.2 cm graphite tubes at room temperature showed nearly complete removal of ozone up to 250 ppb in the Model 202; however, the ozone removal efficiency degraded over several hours as the graphite surface became oxidized. Heating the graphite tubes to 100-130°C resulted in complete recovery of the graphite's reactivity toward ozone but large negative absorbances were observed in the ozone analyzers as the temperature of the graphite scrubber exceeded 145°C. This was due to the emission of various volatile organic hydrocarbons from the graphite tubes as verified by GC-MS. We attribute this to either the thermal breakdown of the organic binder contained in graphite that is added during manufacturing, or to initiation of O_2 oxidation, although the latter is not expected to be significant below about 350°C (Entegris, 2015). Below 135°C, emissions were greatly reduced, and after completing the cleaning process described above, typically resulted in a small negative offset (~ -2 to -5 ppb) that remained constant over time. The exact cause of this small residual negative offset is unclear, although it is likely due to residual organics that are slowly released from the hot graphite. As in the case of conventional ozone scrubbers, this small offset can be incorporated into the calibration parameters of the ozone analyzer.

We conclude that a tube configuration consisting of four 3.175-mm (1/8-in) i.d., 7.62-cm (3-in) long parallel graphite tubes (Figure 1b), which easily fit within the existing Model 202 Ozone Monitor enclosure, provides adequate (> 98%) ozone destruction efficiency comparable with conventional scrubbers. This scrubber has an internal volume of 2.4 cm^3 and geometric surface area of 30.4 cm^2, resulting in a residence time of 0.145 seconds for a typical flow rate of 1 L/min. At a temperature of

100°C and pressure of 1 atm, on average each ozone molecule collides with the surface 1.85×10^4 times while passing through the scrubber. Thus, assuming rapid diffusion to the walls, a collisional reaction probability γ of ~ 1.7×10^{-3} is required to assure >99% ozone destruction. This is similar in magnitude to previously determined probabilities of ozone uptake on fresh carbon soot surfaces (Burkholder et al.,

235   2015). The results discussed in the remainder of this paper were observed with this scrubber design, although the graphite surface area could be increased if necessary. Figure 2 shows examples of calibration plots where the ozone was varied and the graphite scrubber was alternately replaced with a conventional packed-bed Hopcalite scrubber. To test for reproducibility, four different sets of graphite tubes were used within the heater. Slopes of heated graphite vs. Hopcalite ozone measurements ranged

240   from 0.96 to 1.01 among the different sets for concentrations up to 500 ppb of ozone. The overall average slope was 0.98. All calibration plots were highly linear with $R^2 > 0.99$ and their slopes were invariant over the graphite scrubber temperature range of 100-130°C.

3.2   Long-term reliability of the graphite scrubber

245   A primary concern with carbon-based scrubbers is that as the surface of the solid-phase carbon oxidizes, it becomes less reactive toward ozone. In principle, the carbon is oxidized to CO and CO_2, which desorb to the gas phase and are swept away in the case of a flowing analyzer. However, the oxidation to CO and CO_2 in the presence of water vapor typically occurs in several steps through various oxygenated intermediates (i.e., epoxides, alcohols, aldehydes, and ketones), and it is likely that at least

250   some of the carbon lost is in the form of small oxygenated organics such as formaldehyde, acetone and acetaldehyde. These do not present a problem as long as they do not absorb appreciably at 253.7 nm. Ellis and Tometz (1972) were among the first to note that upon exposure to high ozone concentrations, cocoanut charcoal becomes less efficient at removing ozone as it oxidizes. This suggests that oxygenated hydrocarbons on the graphite surface or oxygen functionalities incorporated within the graphite structure

255   have slower ozone reaction rates. A loss in reactivity toward ozone has also been observed for graphite at high (~ 0.5%) levels of ozone (Razumovskii et al., 2007). We also observed this loss in ozone removal efficiency at room temperature and found that heating the graphite scrubber remedies this problem. At elevated temperatures (100°C), continuous exposure of 150 ppb of ozone for 22 hours in the single-beam Model 202 showed no loss of the graphite's ability to destroy ozone.

260   However, incorporation of the graphite scrubber into a dual-beam Model 205 led to unexpected complications. We found that even at 100°C, it was necessary to reduce the flow rate to the minimum required to flush the absorbance cells in order to observe 100% ozone removal. Furthermore, overnight exposure (18 hours) of the graphite tubes to 150 ppb of O_3 in the dual-beam Model 205 resulted in a 10%

loss of the ozone removal efficiency. Exposure to higher ozone concentrations (300-700 ppb) in the dual-
265 beam Model 205 resulted in faster temporal decays which leveled off at ~ 85% ozone removal efficiency
after 2 to 8 hours. The graphite's capacity to destroy ozone could be restored by periodically heating the
graphite to 150°C for 20-30 minutes or by removal of the ozone exposure while continuing with normal
analyzer operation for 3-6 hours. Ellis and Tometz (1972) also had noted that removal of charcoal from
ozone exposure for several hours resulted in a regeneration of the surface reactivity toward ozone.

270 These observations suggest a competition between ozone oxidizing the graphite surface (making
less reactive species at the surface) and loss of these oxidized carbon-containing compounds to the gas
phase (which presumably exposes new, less oxidized surface area). This competition helps explain why
the single-beam Model 202 is less susceptible to losing reactivity toward ozone since the scrubber is only
exposed to ozone flow half of the time (during the I_o measurement). During the I-measurement, there is
275 no flow through the scrubber, but oxidized compounds can still desorb and regenerate the surface. In the
dual-beam monitor, the graphite is continuously exposed to a flow of ozone as it is always directed to one
of the two cells for an I_o measurement. As a result, the surface is being oxidized faster than the graphite
can regenerate. One also expects this competition to be dependent upon the temperature of the scrubber
and the flow rate through it as well as the ozone concentration.

280 Therefore, before the graphite scrubber can be used in long-term continuous monitoring, it is
necessary to fully understand its limitations in terms of its loss of ozone removal efficiency. To further
characterize the graphite scrubber, we undertook extended ambient ozone measurements on the 2B
Technologies roof in Boulder, CO during August and September of 2015. A single-beam Model 202 was
equipped with our heated graphite scrubber (denoted as 202-G) and sampled from the same Teflon inlet
285 line as an FEM (Federal Equivalent Method) Model 205 dual-beam analyzer with a conventional packed-
bed Hopcalite scrubber (205-H). The Model 205 was equipped with Nafion for humidity equilibration;
however, Nafion was removed from the Model 202/graphite scrubber analyzer (humidity interference is
discussed in Section 3.3). Calibrations were performed on both instruments prior to and periodically
throughout the comparison with a Model 306 ozone calibrator. Although the 205-H may be more
290 susceptible to interfering compounds (described in following section), the anticipated bias is < 3 ppb

We initially evaluated the graphite scrubber temperature to 100°C since we had observed no loss
of ozone removal efficiency during lab ozone exposure experiments with our single-beam ozone
instrument. Ambient measurements were made from August 8-24, 2015. Ozone data was averaged to 5
minutes from both instruments (205-H and 202-G) and compared each day. The daily regression slopes
295 were near unity (0.99 ± 0.02) for the first 12 days; however, on the 13th day, comparisons showed that the
202-G analyzer underestimated peak afternoon ambient ozone by ~ 8% and the 202-G continued to drop
over the next three days yielding a regression plot slope of ~ 0.85 versus the 205-H.. This is shown in

Figure 3c, where the slopes of the daily comparison between the 202-G and 205-H are shown as a function of the cumulative ozone exposure (in ppm-hr). The calibration of the 202-G was rechecked and confirmed the scrubber only removed $86 \pm 2\%$ of the ozone passing through it.

The graphite was regenerated by heating to 150°C for 1 hour with no ozone present and the calibration slope returned to 1.01 ± 0.02. The 202-G was then returned to sampling but the graphite scrubber was maintained at 130°C – the highest temperature without inducing significant VOC emission from the graphite tubes as described in Section 3.1. Post-regeneration, the analyzers were compared again from August 24 to September 30, 2015 (38 days). Figure 3a shows a diurnal plot of the ozone measured by the two analyzers on Sept. 26, 2015, near the end of the intercomparison. It is clear from this plot and the regression plot of the same data in Figure 3b that there was excellent agreement between the two instruments. The daily intercomparison slope vs. ozone exposure in Figure 3c confirms there was no graphite scrubber efficiency loss after 38 days (or 30 ppm-hr ozone exposure). A recheck of the analyzer calibrations found them to be within the uncertainty of the initial calibrations. Subsequent measurements using a dual-beam Model 211 equipped with a heated graphite scrubber operating at 130°C indicate that there is also no loss in the ozone removal efficiency after exposure to 20 ppm-hr of ozone. Therefore, it appears the graphite scrubber must be maintained at temperatures greater than 100°C for reliable long-term continuous monitoring. A temperature of 130°C appears to be optimal for maintaining the balance between oxidation of the graphite by ozone and the loss of oxidized carbon from the surfaces to regenerate fresh carbon.

3.3 Interference testing

As mentioned earlier, carbon-based scrubbers (typically charcoal or activated carbon) remove ozone from air, but they also effectively remove many other species such as VOCs and water and thus would introduce interferences in ozone measurements. However, the more ordered planar structure of graphite and the greatly reduced surface area provide fewer sites for adsorption of interfering species. The results of our interference testing described below were performed with the graphite scrubber heated to 100°C. Heating the graphite scrubber to 130°C (the more optimal temperature found in our subsequent longevity testing described in the previous section) would likely reduce adsorption of water, mercury and aromatic VOCs. Hence, these results can be viewed as a conservative estimate of the expected behavior of the graphite scrubber in reducing interferences in ozone measurements.

3.3.1 Water vapor

Previous studies have shown that rapid humidity changes can cause large apparent ozone absorptions (equivalent to tens of ppb) in most commercial ozone analyzers (Kleindeinst et al., 1993; Wilson and Birks, 2006; Spicer et al., 2010). Wilson and Birks (2006) explained this behavior as being

due to changes in the refractive index at the surface of the optical cell resulting from varying amounts of water vapor adsorbed to cell walls. Initial experiments with a Model 202 analyzer equipped with a conventional Hopcalite scrubber but no Nafion tube, indicated large signal changes coinciding with changes in humidity (Figure 4, black dashed line).   A large positive interference was observed as humidity was rapidly increased (uptake of water by the scrubber) and an opposite negative interference seen upon changing from humid to drier air (release of water from the scrubber). Figure 4 (magenta line) confirms that placement of a Nafion tube at the entrance to the optical cell to equilibrate the humidity with surrounding air (same humidity for I and I_o) effectively eliminates the water vapor interference, as shown earlier by Wilson and Birks (2006). A drawback of this approach is that Nafion tubing is expensive, and the length of tubing required to attain adequate equilibration can place limits on its use in miniaturized analyzers or can introduce flow restrictions, thus making it impractical in some applications.

The graphite scrubber proposed also mitigates artefacts caused by changing water vapor concentrations. As seen in Figure 4, the initial large change in humidity does cause an apparent absorption of ~ 10 ppb of "O_3" with the graphite scrubber in-line. It appears that some water is initially taken up by the graphite, likely due to the somewhat porous nature of the graphite structure. However, water content within the graphite scrubber equilibrates within about 2 minutes and returns to its original value, whereas the Hopcalite trap remains compromised for > 15 minutes. Subsequent removal of the high water vapor concentration leads to a negative response as water vapor desorbs from each scrubber. But again, the recovery of the graphite scrubber is relatively rapid compared to the Hopcalite, so although there is some water uptake, equilibration is rapid enough to exceed typical humidity changes and 30-60 minute ozone averages will be relatively unaffected.

Variation of relative humidity did indicate a slight water dependency in the graphite scrubber and exhibited some differences between different graphite tubes. Figure 5 illustrates this behavior, showing two different sets of graphite tubes (4 tubes in parallel, 3-in long). Set #1 indicated about a +2.5 ppb change from dry to near-saturated air; whereas Set #2 was essentially independent of the humidity. Given graphite's hydrophobic nature, these differences are perplexing, but could be due to differing degrees of oxidation on the graphite surface or on binders within the graphite, making the surface slightly more hydrophilic. The graphite scrubber's low sensitivity to humidity was also confirmed in our ambient measurements (Section 3.2) where we observed no correlation between ambient humidity changes and concentration differences between the graphite equipped Model 202-G and the Hopcalite and Nafion equipped Model 205-H.

3.3.2 Mercury

Gaseous elemental mercury concentrations are typically less than a few ppt in ambient air, but mercury poses a problem in ozone photometers because typically the Hg atomic absorption line is used as

the photometer's excitation source (Hg line at 253.7 nm). Birks et al. (2009) estimate that common ozone photometers could be 1860 times more sensitive to elemental mercury than ozone (Selectivity = 1.86 ppb O_3/ppt Hg) depending on how efficiently the scrubber removes mercury. Recent measurements in our laboratory showed that mercury absorbs ~1350 times more strongly than ozone in the Model 202 Ozone Monitor using the packed-bed Hopcalite scrubber (Birks, 2016 unpublished data). There is also evidence suggesting that the efficiency of mercury uptake in several conventional scrubbers may depend on humidity (U.S-EPA, 1999; Spicer et al., 2010), implying that these may act as a temporary reservoir capable of releasing mercury at later times following humidity changes.

In order to examine possible interferences due to elemental mercury, varying concentrations of mercury vapor were added to the Model 202 ozone monitor and responses were monitored (in apparent ppb of ozone) while the various graphite and conventional scrubbers were interchanged. As we did not have an independent measurement of mercury vapor concentrations, all measurements were made relative to the conventional packed-bed Hopcalite scrubber used in the 2B Technologies analyzers. For different levels of mercury additions, Figure 6 shows the apparent ozone measured by the photometer as various scrubbers were alternated with the packed-bed Hopcalite. Five different sets of graphite tubes (set = 4 tubes in parallel, each 3-in long) were tested and the slopes of plots of apparent ozone concentration vs. those obtained for the Hopcalite scrubber ranged from < 0.01 to 0.03 (median set is shown in Figure 6). One set showed no measurable response to mercury up to an apparent ozone concentration of 2,200 ppb for the Hopcalite scrubber. Noting above our recent observation that mercury absorbs 1350-fold stronger than ozone (or 1.35 ppb O_3/ppt Hg), this leads to a response ratio of $\leq$ 0.04 ppb O_3/ppt Hg for the graphite scrubber. Measurements made at 22% and 80% RH exhibited no differences (Figure 6). In addition, measurements made with and without Nafion tubing inserted before the optical cell gave identical results, suggesting that mercury is neither lost nor interacts significantly with Nafion.

The heated silver wool scrubber exhibited the largest mercury response, with a slope slightly greater than unity compared to Hopcalite (Fig. 6). Silver is known to rapidly form an amalgam with mercury (Dumarey et al., 1985) which likely explains this large response. Previous studies have shown that both the 2B Technologies Hopcalite scrubber and heated silver wool scrubber remove mercury vapor efficiently – reporting response ratios between 0.6 to 1.1 ppb O_3/ppt Hg (Spicer et al., 2010; U.S.-EPA, 1999). We report a response ratio of 1.49 ppb O_3/ppt Hg for the heated silver wool assuming 1.35 ppb O_3/ppt Hg for the Hopcalite scrubber – approximately 1/3 higher than the previous studies. The sensitivity to Hg depends on the width of the emission line of the lamp (Birks et al., 2009), which may vary from instrument to instrument.

Both the Teledyne-API and Thermo Electron scrubbers use screens coated with MnO_2 and showed less interference from mercury vapor compared to the packed-bed Hopcalite scrubber (slopes of

400   0.18, and 0.065). This yields response ratios of 0.24 and 0.09 ppb O_3/ppt Hg for the Teledyne-API and

Thermo Electron scrubbers, respectively.   Smaller responses are likely due to the large reduction in

scrubber surface area by use of the coated screens. Measurements made at both high ($\geq 80\%$) and low

(20%) relative humidity showed no significant differences, although the considerable scatter in the data

likely obscures any small humidity dependencies. The interference of mercury in ozone photometers with

405   MnO_2-based scrubbers has been the subject of several previous investigations. The U.S.-EPA (1999)

reported response ratios in the range 0.12 to 0.24 ppb O_3/ppt Hg using a Thermo Electron scrubber. This

study also suggested a lowering of the response ratio with increasing humidity. Higher response ratios

(0.87 and 0.6 ppb O_3/ppt Hg) have also been reported in dry air (Li et al., 2006; Spicer et al., 2010).

Spicer et al. (2010) also reported that the response ratio decreased by a factor of 2 when using humidified

410   air (RH ~ 80%), which is closer to both our results and those of the EPA. As will be shown for VOCs in

the next section, it is likely that even a small amount of water vapor can make a significant change in the

adsorption properties of these solid-phase scrubbers; thus the higher response ratios determined in dry air

may not be applicable to sampling of ambient air. The use of a heated graphite scrubber can reduce the

interference in ozone photometers from mercury vapor by a factor of ≥ 30 over the packed-bed Hopcalite

415   scrubber and by a factor of ≥ 2 over the best solid-phase scrubber.

        This low response ratio is only matched by using the gas-phase nitric oxide (NO) titration as a

means of scrubbing ozone. In the recently introduced 2B Technologies Model 211 Scrubberless Ozone

Monitor[TM], gas-phase NO titration eliminates the need for a solid-phase scrubber, and effectively

eliminates interferences from both UV-absorbing species and water vapor (Birks et al., 2013). However,

420   a source gas of NO is required, reducing the portability of the instrument and adding long-term cost. The

heated graphite scrubber avoids these disadvantages.

        In general, mercury is not expected to be a significant interference in outdoor ambient air.

Although there are some elevated measurements of mercury vapor in urban areas of Asia (up to ~ 3 ppt:

Fang et al., 2004; Liu et al., 2002; Kim and Kim, 2002), concentrations typically range from 0.2

425   (background) to 0.5 (urban) ppt (Obrist et al., 2008; Weiss-Penzias et al., 2003; Denis et al., 2006).

However gas-phase mercury can reach higher levels near industrial or mining sources. Elevated mercury

levels have also been shown to be present for indoor air (Carpi and Chen, 2001; Garetano et al., 2006).

Because indoor ozone concentrations are typically low (~ 20-80% of outdoor air, U.S. EPA, 2016),

mercury poses a larger potential problem for indoor air quality monitoring of ozone. For example, Carpi

430   and Chen (2001) report indoor mercury concentrations of up to 520 ng m^{-3} (~ 63 ppt). This would

correspond to measured absorbances equivalent to ~ 85 ppb O_3 with the packed-bed Hopcalite, ~ 6-15

ppb O_3 with conventional MnO_2 screens, and < 2.6 ppb O_3 using the heated graphite.

3.3.3 Volatile Organic Compounds (VOCs)

Interferences from volatile organic compounds are more complicated due to the wide variety of compounds and their properties. There are many diverse atmospheric VOCs having a wide range of 253.7 nm absorption cross sections, volatilities, and potential responses to humidity. Along with the VOC absorption cross sections, Table 1 also lists room temperature vapor pressures as an indicator of volatility. Aromatic VOCs are the most important when discussing interferences in ozone monitors since the conjugation between the carbon-carbon double bonds both shifts the absorption spectrum to longer wavelengths and results in larger UV cross sections. Addition of various functional groups (hydroxyl, aldehyde, nitro, etc.) to the aromatic ring can further increase the absorption cross section. Furthermore, substitutions often result in lower volatility, making these species more likely to be retained in a solid-phase scrubber.

Interferences from VOCs typically result from two different mechanisms: (1) adsorption of the compound by the scrubber, resulting in a positivebias, and (2) subsequent later desorption of that compound from the scrubber due to eventual elution and/or changes in temperature or humidity that yield a negative bias. These two processes are complex functions of environmental conditions (temperature and humidity), volatility and chemical properties of the specific VOC, as well as the reactivity and surface area of the scrubber material.

Past studies of VOC interferences have typically been of three types: (1) measurement of total net ozone biases during irradiation of simulated atmospheres in smog chambers (Kleindeist et al., 1993; Leston et al., 2005); (2) simultaneous atmospheric measurements by different analyzers using different measurement techniques (Ollison et al., 2013; Dunlea et al., 2006); and (3) addition of selected VOCs to ozone analyzers to determine the interference from that particular VOC (Grosjean and Harrison, 1985; Spicer et al., 2010). All of these approaches contribute to our understanding of the significance of VOC interferences in ozone monitors; however, we have chosen the latter approach to initially evaluate our heated graphite scrubber because it is a more direct approach and reproducible signals can be easily quantified. We chose p-xylene, phenol, p-tolualdehyde, and o-nitrophenol, as test VOCs since they have reported 253.7-nm absorption cross sections ranging from 5×10^{-19} (p-xylene) to 2.15×10^{-17} (o-nitrophenol) cm^2 molecule^{-1} (Keller-Rudek et al., 2013) and vapor pressures (25°C) of 0.11 to 8.8 mm Hg.

VOC Interferences in Dry Air. Initial experiments examined VOC interferences in dry air (RH < 3%) in the absence of ozone using a single-beam Model 202 monitor equipped with the various scrubbers described above. No Nafion tubing was installed upstream of the optical cell in the monitor. VOC concentrations were measured by sampling the same air stream into the inlet of a GC-FID. Upon VOC addition, apparent ozone absorbances were observed to reach steady values within the initial 2-4 minutes

with both the Hopcalite and MnO₂-based scrubbers. With the heated graphite scrubber, there was a rapid increase in apparent ozone upon addition, followed by a decay to steady values after 3 minutes. Average

470   apparent ozone concentrations were obtained after 5 minutes of exposure and plotted vs. VOC concentrations measured with the GC-FID (Figure 7). There were no signs of surface saturation effects, as indicated by the linearity of the apparent ozone with VOC concentration plots. For all the compounds tested, the heated graphite scrubbers showed less apparent ozone. The slopes of the plots in Figure 7 are given in Table 2. In all cases, the slopes were a factor of 2.5 to 20 less for the graphite scrubber than for

475   Hopcalite or the MnO₂ scrubbers, indicating greatly reduced VOC uptake by the graphite. Data from two sets of graphite tubes (4 tubes in parallel) gave identical results for both p-xylene and phenol; however, both p-tolualdehyde and o-nitrophenol did exhibit slightly different apparent ozone values from these two different sets of graphite tubes. Responses for three other sets of graphite tubes were also tested against the Hopcalite scrubber and gave absorbances within the range of those shown in the figure. It remains

480   unclear why different tube sets show slightly different behavior, but, again, it likely lies in the degree of graphite surface oxidation.

In dry air both Hopcalite and MnO₂ scrubbers exhibited similar responses for all the compounds tested. If the scrubbers remove 100% of the VOC compound, then the slope of these plots should be the inverse of the selectivity ratio reported in Table 1:

485
$$\frac{1}{S} = Slope = \frac{\sigma_{VOC-254nm}}{\sigma_{O3-254nm}} \text{ (in ppb O}_3\text{/ppb VOC)} \tag{2}$$

There is good agreement in the theoretical slope and that observed for p-xylene (see Table 2), suggesting both Hopcalite and MnO₂-based scrubbers effectively scavenge all of the p-xylene in dry air. However, the slopes for phenol, p-tolualdehyde, and o-nitrophenol were all significantly higher by factors of 1.4, 3.3, and 4.1, respectively, than those computed from previously reported absorption cross sections. As

490   this would require >100% removal by the scrubber, this can only be explained either by errors in the previously reported VOC cross sections or an underestimation in the VOC concentrations via the GC technique. Since the error tends to decrease with volatility, the latter is more likely as it becomes more difficult to quantitatively desorb the VOC from the Tenax pre-concentration trap used in the GC. Furthermore, if our o-nitrophenol concentrations were correct, this suggests a 253.7-nm absorption cross

495   section of nearly 9×10^{-17} cm² molecule⁻¹ which seems inexplicably large.

We did not pursue a more accurate GC-FID VOC quantitation as the heated graphite scrubber can still be assessed on a relative basis to the conventional scrubbers from the ratios of the slopes in Figure 7. Assuming that the packed bed Hopcalite scrubber exhibits the theoretical selectivity factor based on absorption cross sections for each VOC tested (reported in Table 1), selectivity ratios of 83, 28, ≥ 12, and

500   ≥ 1.5 ppb VOC/ppb O₃ were estimated for p-xylene, phenol, p-tolualdehyde, and o-nitrophenol,

respectively, for the heated graphite scrubber. In other words, it would require a p-xylene concentration of 83 ppb to produce a signal of 1 ppb O_3 in an analyzer using a heated graphite scrubber compared to a concentration of 20 ppb for the Hopcalite or MnO_2 scrubbers.

505   We observed less than 10% difference between the response ratios obtained with the Hopcalite and the two MnO_2 thin-film screen scrubbers for both p-tolualdehyde and o-nitrophenol in dry air. Spicer et al. (2010) report values of 0.8 and 0.0 to 0.5 ppb O_3/ppb p-tolualdehyde in dry air when using the MnO_2 and Hopcalite scrubbers, respectively, a difference of $\geq 30\%$. They also report values of 2.2 and 1.1 to 1.8 ppb O_3/ppb o-nitrophenol for the MnO_2 and Hopcalite scrubbers. This leads to differences ranging from 20% to a factor of two, contrary to that observed in the current study. However,

510   concentration levels of interfering VOCs were quite low in the Spicer et al. (2010) study, ranging from 7.6 to 14 ppb and their measured apparent ozone mixing ratios were < 15 ppb. At these levels, small signal drifts, or the typical precision of ± 1 to 2 ppb in the ozone analyzers impart significant uncertainty in the measured response ratio. It should be noted that the value of 0.8 ppb O_3/ppb p-tolualdehyde reported in Spicer et al. (2010) for the MnO_2 scrubber is also above the maximum theoretical response

515   based on the reported absorption cross sections by a factor of 1.7 (1/S = 0.48, Table 1).

Zdanevitch (2002) reported a higher response for phenol and other VOCs studied with ozone present and suggested that photochemical production of stronger-absorbing compounds within the optical cell may be responsible. Our experiments with p-tolualdehyde and p-xylene failed to show such evidence for photochemical behavior. Absorbances recorded with both ozone and VOC present were equivalent to

520   the sum of the absorbances when these components were measured individually within the precision of the analyzer. This supports calculations that suggest negligible photochemistry can occur due to the low photon flux and short residence time in the 2B Technologies Model 202.

VOC interferences in humid air. Even at low humidity levels, water vapor is adsorbed to some extent by most of the conventional solid-phase scrubbers. This changes the surface characteristics of the

525   solid phase which, in turn, can alter the adsorption and desorption of other compounds. This is also dependent upon the properties of the species of interest – especially the particular compound's volatility. For the most volatile compound studied, p-xylene, even low levels of humidity caused the observed interference (apparent ozone) to decrease over time. Figure 8a shows the temporal behavior of the apparent ozone absorption upon addition of ~ 1 ppm of p-xylene in moderately humid ozone-free air with

530   an analyzer equipped with a conventional packed-bed Hopcalite scrubber and Nafion. There is an initial spike in the signal that then decays over time. The inset of Figure 8a shows how this decay varied as a function of RH. In each case, p-xylene was added to generate an apparent ozone signal of ~ 80 ppb in dry air. The humidity was then changed within 20 seconds and the absorbance decay was recorded. The

apparent ozone decay was faster at higher humidity, suggesting that the presence of water causes less p-

535 xylene to be retained in the scrubber.

However, even at these higher water vapor concentrations the scrubber still accumulated p-xylene. This is apparent upon turning off the p-xylene source, as a large negative absorbance was then observed (Figure 8a). p-Xylene was now slowly desorbing from the scrubber material, thus absorbing more light during the I_o measurement relative to I. This slow emission was also humidity dependent –

540 becoming faster at higher relative humidity (data not shown). Scrubbers from the Thermo Electron and Teledyne-API instruments show similar behavior except that the time response is much faster ($<$ 2 min., Figure 8a), presumably due to the lower surface area of scrubber material. In fact, these scrubbers were observed to pass p-xylene nearly quantitatively, similar to the graphite scrubber after about 5 minutes as long as RH $>$ 10%. These scrubbers also showed rapid release of the p-xylene once the VOC exposure

545 was discontinued. However, the equilibration is rapid enough that, even at low humidity, the effect of xylenes on hourly averaged ambient ozone measurements is likely negligible with these low surface area scrubbers.

VOC responses with the heated graphite scrubber tend to be relatively insensitive to changes in relative humidity. Figure 9 shows a 1 ppm p-xylene addition to an ozone analyzer initially equipped with

550 a Hopcalite scrubber at low RH (9 %), giving an apparent O_3 concentration of 67 ppb. The Hopcalite was then exchanged for a heated graphite scrubber and the relative humidity varied over the following 95 minutes where there is little to no RH-driven change in the observed absorbance. A plot of the averaged signal versus relative humidity yields a slope of 0.018 ppb apparent O_3/% RH, where a humidity change from 20 to 80% only alters the apparent ozone signal from 1 ppm of p-xylene by +1 ppb.

555 As the VOC becomes less volatile, the advantages of the heated graphite scrubber become more significant. Experiments with p-tolualdehyde indicated that a small amount of humidity (RH = 22%) did not alter the behavior from that observed in dry air for any of the various scrubbers. However, as RH increased to 75%, the coated MnO_2 screen scrubbers showed a large increase, followed by a slow decay over 20-30 minutes (Figure 8b) – behavior akin to the packed-bed Hopcalite/p-xylene exposure discussed

560 previously. These scrubbers also exhibited a larger negative absorbance when the p-tolualdehyde flow was removed indicating release of adsorbed p-tolualdehyde post-exposure, similar to the Hopcalite/p-xylene temporal profiles. For phenol, the selectivity for both the Hopcalite and MnO_2 scrubbers remained constant regardless of humidity (data not shown). Even at RH = 75%, the Hopcalite and MnO_2 scrubbers behaved similar to dry air, quantitatively removing phenol and showing no decay in the apparent O_3

565 absorbance over at least 10 minutes. We did not examine the behavior of o-nitrophenol with humidity, but presume it would be similar to that of phenol.

Although the conventional MnO$_2$ scrubbers with low surface area appear to be compatible with the more volatile aromatics like xylene, their propensity to have uptake and re-emission of less volatile compounds dependent upon humidity levels is problematic in estimating ozone monitor biases. The selectivity ratio described above is now a function of humidity which varies in time. The wide variety of different atmospheric VOCs and their varying properties suggest that it will be nearly impossible to quantitatively model or estimate whether these scrubbers are consuming or releasing compounds, i.e., whether ozone monitors are biased negatively or positively. For example, Spicer et al. (2010) reported a decrease in the percent response ratio for the MnO$_2$ scrubber from 0.8 to 0.1 ppb p-tolualdehyde/ppb O$_3$ going from dry to humid air. This lowering of the p-tolualdehyde absorbance with RH was also observed in this study, but was dependent upon exposure time such that a single selectivity ratio cannot be used. In contrast to the conventional solid-phase scrubbers, VOC interferences observed with the heated graphite scrubber are virtually insensitive to humidity changes for all the compounds studied. Although the graphite scrubber does retain a small fraction of the VOCs, the lack of a humidity dependence makes potential ozone monitor biases easier to predict.

4   Conclusions

A new solid-phase scrubber based on graphite for use in conventional ozone photometers was investigated and found to effectively remove ozone, while offering significant advantages over current ozone scrubbers with regard to species that typically interfere in ozone measurements. When heated to 100-130°C, the graphite scrubber quantitatively removed ozone up to 500 ppb – well above the concentration levels required for most ambient or indoor monitoring studies. After two weeks of ambient measurements in a single-beam instrument slow oxidation of the graphite surface reduced its ability to completely remove ozone when operated at the lower end of the temperature range studied (≤ 100°C). However, when operated at 130°C, no loss of ozone removal efficiency was observed up to exposures of 30 ppm-hr over 38 days, and agreement with a conventional FEM analyzer was excellent throughout the time period. The higher temperature likely facilitates removal of lower reactivity oxidized species from the graphite surface either by enhancing desorption or the reaction rate with ozone. Therefore, long-term measurements require continuous operation near the maximum of 130°C or periodic regeneration of the scrubber by heating it to 150°C for 20-30 minutes. These conditions appear to be valid for both single-beam and dual-beam monitors.

The major advantage of the heated graphite scrubber is its ability to pass many of the known atmospheric interferences that plague conventional solid-phase ozone scrubbers. Elimination of small biases of a few ppb of ozone can be critical in marginal compliance situations where ambient ozone is near the NAAQS. Water effects on ozone measurements (through refractive index changes in the optical

cell) were virtually eliminated by use of the graphite scrubber, thereby eliminating the need for humidity

equilibration using Nafion. Gas-phase mercury interference was ≤ 3% of a packed-bed Hopcalite

scrubber, and at least a factor of two better than other conventional MnO_2 coated-screen scrubbers. The

graphite scrubber was also observed to consistently exhibit smaller interferences in dry air for a series of

605   substituted aromatic compounds ranging in volatility and extinction coefficient. The apparent ozone

absorptions measured with the graphite scrubber were typically a factor of 2.5 to 20 smaller than those

with the conventional Hopcalite or MnO_2 scrubbers. Our results suggest that to generate an absorbance

equivalent to 1 ppb of ozone would necessitate concentrations of 83 ppb of p-xylene, 28 ppb of phenol, ≥

12 ppb of p-tolualdehyde, ≥ 1.5 ppb of o-nitrophenol, or ≥ 25 ppt of mercury vapor. These are nearly

610   three or more times greater than typical ambient concentrations for any of these species (Table 1).

The small VOC interference observed with the graphite scrubber was also insensitive to humidity

level. Although the conventional commercial solid-phase scrubbers tended to remove all of the aromatic

VOCs studied in dry air, these scrubbers tended to show less interferences at higher humidity levels (i.e.,

less aromatic compounds retained in the scrubber). This lowering of the interference was tied to the

615   particular VOC's intrinsic volatility and the surface area of the solid phase scrubber. Low volatility

compounds (such as phenol) were retained regardless of humidity level, whereas compounds with higher

volatility (p-xylene) were nearly quantitatively passed by the scrubbers using coated screens with low

surface area. For compounds that were intermediate in volatility, such as p-tolualdehyde, the

conventional commercial scrubbers quantitatively removed the VOC at low humidity (< 40% RH), but

620   the coated-screen scrubbers showed a slow equilibration at high water vapor concentrations (> 70% RH,

t_{equil} ~ 30 min.). These also released p-tolualdehyde upon ending exposure to the compound. These

results strongly suggest that these scrubbers tend to accumulate VOC under drier conditions (creating a

positive bias in ozone analyzers) and then subsequently re-release them as humidity is increased (creating

the possibility of a negative bias). This complex behavior involving humidity and volatility is avoided by

625   use of the heated graphite scrubber.

Although more work is needed to determine whether the graphite scrubber can replace

conventional solid-phase scrubbers for long-term compliance monitoring, both the lab and field studies

presented here suggest that the heated graphite scrubber has the potential to provide more accurate ozone

concentration measurements by reducing conventional photometer susceptibility to many common

630   interferences. The operating characteristics (flow, pressure, etc.) of the heated graphite scrubber are also

compatible with most conventional ozone monitors. Reducing interferences in ozone measurements is

especially important for ozone monitoring in highly polluted regions or in applications where high levels

of VOCs or mercury exist such as in smog chamber experiments, indoor environments, or near areas of

mercury contamination. It may also prove to be important in areas of marginal non-compliance with

635   ambient ozone standards.

5   Acknowledgements

The authors would like to acknowledge Dr. John Ortega at the National Center for Atmospheric Research for assistance with GC/FID measurements. We would also like to thank Dr. Will Ollison for his advice

640   and critique of this manuscript.

6   References

Avnery, S., Mauzerall, D.L., Liu, J., and Horowitz, L.W.: Global crop yield reductions due to surface ozone exposure: 1. Year 2000 crop production losses and economic damage, Atmos. Environ., 45, 2284-

645   2296, 2011.

Bernardo-Bricker, A., Farmer, C. Milne, P., Riemer, D., Zika, R., and Stoneking, C.: Validation of speciated nonmethane hydrocarbon compound data collected during the 1992 Atlanta Intensive as part of the Southern Oxidants Study, J. Air and Waste Manage. Assoc., 45, 591-603, 1995.

650
Birks, J.W., Williford, C.J., and Andersen, P.C.: Use of a Broad Band UV Light Source for Reducing the Mercury Interference in Ozone Measurements, U.S. Patent Application US 2009/0302230 A1, 2009.

Birks, J.W., Andersen, P.C., and Williford, C.J.: Ozone monitor with gas-phase scrubber, U.S. Patent US

655   8,395,776 B2, Mar. 12, 2013.

Birks, J.W., Turnipseed, A.A., Andersen, P.C., and Williford, C.J.: Heated Graphite Scrubber to Reduce Interferences in Ozone Monitors, U.S. Patent US 2016/0025696 A1, Jan. 28, 2016.

660   Burkholder, J.B., Sander, S.P., Abbatt, J., Barker, J.R., Huie, R.E., Kolb, C.E., Kurylo, M.J., Orkin, V.L., Wilmouth, D.M., and Wine, P.H.: Chemical Kinetics and Photochemical Data for Use in Atmospheric Studies, Evaluation No. 18, JPL Publication 15-10, Jet Propulsion Laboratory, Pasadena, 2015.

Burnett, R.T., Brook, J.R., Yung, W.T., Dales, R.E., and Krewski, D.: Association between ozone and

665   hospitalization for respiratory diseases in 16 Canadian cities, Environ. Res., 72, 24-31, 1997.

Carpi, A., and Chen, Y.F.: Gaseous elemental mercury as an indoor air pollutant, Environ. Sci. Technol., 35, 4170-4173, 2001.

670   Chameides, W.L., and Walker, J.C.G.: A photochemical theory of tropospheric ozone, J. Geophys. Res., 78, 8751-8759, 1973.

Davies, L.: Nitrobenzene, International Programme on Chemical Safety - Environmental Health Criteria 230, World Health Organization, 2003.

675
Delhomme, O., Morville, S. and Millet, M.: Seasonal and diurnal variations of atmospheric concentrations of phenols and nitrophenols measured in the Strasborg area, France, Atmos. Pollution Res., 1, 16-22, 2010.

680   Denis, M.St., Song, X., Lu, J.Y., and Feng, X.: Atmospheric gaseous elemental mercury in downtown Toronto, Atmos. Environ, 40, 4016-4024, 2006.

Dumarey, R., Dams, R., and Hoste, J.: Comparison of the collection and desorption efficiency of activated charcoal, silver and gold for the determination of vapor-phase atmospheric mercury, Anal.
685   Chem., 57, 2638-2644, 1985.

Dunlea, E.J., Herndon, S.C., Nelson, D.D., Volkamer, R.M., Lamb, B.K., Allwine, E.J., Grutter, M., Ramos-Villegas, C.R., Marquez, C., Blanco, S., Cardenas, B., Kolb, C.E., Molina, L.T., and Molina, M.J.: Technical note: Evaluation of standard ultraviolet absorption ozone monitors in a polluted urban
690   environment, Atmos. Chem. Phys., 6, 3163-3180, 2006.

Eiguren-Fernandez, A., Miguel, A.H., Foines, J.R., Thurairatnam, S., and Avol, Ed. L.: Seasonal and spatial variation of polycyclic aromatic hydrocarbons in vapor-phase and PM2.5 in Southern California urban and rural communities, Aer. Sci. and Technol., 38, 447-455, 2004.
695

Ellis, W.D., and Tometz, P.V.: Room-temperature catalytic decomposition of ozone, Atmos. Environ., 6, 707-714, 1972.

Emberson, L., Ashmore, M., and Murray, F.: Air Pollution Impacts on Crops and Forests. A Global
700   Assessment, Imperial College Press, London, U.K., 2003.

Emberson, L.D., Büker, P., Ashmore, M.R., Mills, G., Jackson, L.S., Agrawal, M., Atikuzzaman, M.D., Cinderby, S., Engardt, M., Jamir, C., Kobayashi, K., Oanh, N.T.K., Quadir, Q.F., and Wahid, A.: A comparison of North American and Asian exposure–response data for ozone effects on crop yields,
705   Atmos. Environ., 43, 1945-1953, 2009.

Entegris, Properties and characteristics of graphite, accessed at:
https://www.entegris.com/content/dam/web/resources/manuals-and-guides/manual-properties-and-characteristics-of-graphite-109441.pdf , 2015.
710

Fang, F., Wang, Q., and Li, J.: Urban environmental mercury in Changchun, a metropolitan city in Northeastern China: Source, cycle, and fate, Science of the Total Environ., 330, 159-170, 2004.

715   Finlayson-Pitts, B.J. and Pitts, J.N.: Chemistry of the Upper and Lower Atmosphere: Theory, Experiments and Applications, Academic Press, San Diego, 2000.

Garetano, G., Gochfeld, M., and Stern, A.H.: Comparison of indoor mercury vapor in common areas of residential buildings with outdoor levels in a community where mercury is used for cultural purposes,
720   Environ. Health Perspect., 114, 59-62, 2006.

Greenberg, J.P., Lee, B., Helmig, D., and Zimmerman, P.R.: Fully automated gas chromatograph-flame ionization detector system for the in situ determination of atmospheric non-methane hydrocarbons at low parts per trillion concentration, J. Chrom. A., 676, 389-398, 1994.
725

Griffin, R. J., Cocker, D. R., Flagan, R. C., and Seinfeld, J. H.: Organic aerosol formation from the oxidation of biogenic hydrocarbons, J. Geophys. Res., 104(D3), 3555–3567, 1999.

Grosjean, D., and Harrison, J.: Response of chemiluminescent NOx analyzers and ultraviolet ozone
730   analyzers to organic air pollutants, Environ. Sci. Technol., 19, 862-865, 1985.

Haagen-Smit, A.J., and Fox, M.M.: Photochemical ozone formation with hydrocarbons and automobile exhaust, J. Air Pollut. Control Assoc., 4, 105-108, 1954.

735   Hennig, G.R.: Anisoptropic reactivities of graphite – I. Reactions of ozone and graphite, Carbon, 3, 107-114, 1965.

Huntzicker, J.A., and Johnson, R.L.: Investigations of an ambient interference in the measurement of ozone by ultraviolet photometry, Environ. Sci. Technol., 13, 1414-1416, 1979.
740

Keller-Rudek, H., Moortgat, G.K., Sander, R., and Sörensen, R.: The MPI-Mainz UV/VIS spectral atlas of gaseous molecules of atmospheric interest, Earth Syst. Sci. Data, 5, 365-373, 2013.

Kim, K.H., and Kim, M.Y.: A decadal shift in total gaseous mercury concentration levels in Seoul,
745   Korea: changes between the late 1980s and the late 1990s: Atmos. Environ., 36, 663-675, 2002.

Kleindienst, T.E., Hudgens, E.E., Smith, D.F., McElroy, F.F., and Bufalini, J.J.: Comparison of chemiluminescence and ultraviolet ozone monitor responses in the presence of humidity and photochemical pollutants, J. Air Waste Manage. Assoc., 43, 213-222, 1993.
750

Lee P., and Davidson, J.: Evaluation of activated carbon filters for removal of ozone at the ppb level, J. Am. Ind. Hyg., 60, 589-600, 1999.

Lee, A., Goldstein, A. H., Keywood, M. D., Gao, S., Varutbangkul, V., Bahreini, R., Ng, N. L., Flagan,
755   R. C., and Seinfeld, J. H.: Gas-phase products and secondary aerosol yields from the ozonolysis of ten different terpenes, J. Geophys. Res., 111, D07 302, doi:10.1029/2006JD007050, 2006.

Leston, A.R., Ollison, W.M., Spicer, C.W., and Satola, J.: Potential interference bias in ozone standard compliance monitoring, J. Air Waste Manage. Assoc., 55, 1464-1472,
760   doi:10.1080/10473289.2005.10464749, 2005.

Li, Y., Lee, S.-R., and Wu, C.-Y.: UV-absorption-based measurements of ozone and mercury: an investigation on their mutual interferences, Aerosol Air Quality Res., 6, 418-429, 2006.

765   Liu, S., Nadim, F., Perkins, C., Carley, R.J., Hoag, G.E., Lin, Y., and Chen, L.: Atmospheric mercury monitoring survey in Beijing, China, Chemosphere, 48, 97-107, 2002.

Mahmoud, F.M., Kang, D. and Aneja, V.P.: Volatile organic compounds in some urban locations in the United States, Chemosphere, 47, 863-882, 2002.
770

McCarthy, J.E. and Lattanzio, R.K.: Ozone Air Quality Standards: EPA's 2015 Revision, Congressional Research Reports Publication #R43092, 2016.

Meyer, C.P., Elsworth, C.M., and Galbally, I.E.: Water vapor interference in the measurement of ozone in
775   ambient air by ultraviolet absorption, Rev. Sci. Instrum., 62, 223-228, 1991.

Obrist, D., Hallar, A.G., McCubbin, I., Stephens, B.B., and Rahn, T.: Atmospheric mercury concentrations at Storm Peak Laboratory in the Rocky Mountains: Evidence for long-range transport from Asia, boundary layer contributions, and plant mercury uptake, Atmos. Environ., 42, 7579-7589,
780   2008.

Ollison, W.M., Crow, W., and Spicer, C.W.: Field testing of new technology ambient air ozone monitors, J. Air Waste Manage. Assoc., 63, 855-863, doi:10.1080/10962247.2013.796898, 2013.

785   Parrish, D.D. and Fehsenfeld, F.C.: Methods for gas-phase measurements of ozone, ozone precursors and aerosol precursors, Atmos. Environ. 34, 1921-1957, 2000.

Razumovskii, S.D., Gorshenev, V.N., Kovarskii, A.L., Kuznetsov, A.M., and Shchegolikhin, A.N.: Carbon nanostructure reactivity: Reactions of graphite powders with ozone, Fullerenes, Nanotubes and 790   Carbon Nanostructures, 15, 53-63, 2007.

Ryerson, T.B., Buhr, M.P., Frost, G.J., Goldan, P.D., Holloway, J.S., Hubler, G., Jobson, B.T., Kuster, W.C., McKeen, S.A., Parrish, D.D., Roberts, J.M., Sueper, D.T., Trainer, M., Williams, J. and Fehsenfeld, F.C.: Emissions lifetimes and ozone formation in power plant plumes, J. Geophys. Res., 795   103, 22569-22583, 1998.

Saathoff, H., Kamm, S., Möhler, O., Naumann, K.-H., and Schurath, U.: Kinetics and Mechanism of the Heterogeneous Interaction of Ozone with Soot Aerosol, J. Aerosol Sci., 29, S889-S890, 1998.

800   Seila, R.L., Lonneman, W.A. and Meeks, S.A.: Determination of C2 to C12 ambient air hydrocarbons in 39 U.S. cities from 1984 through 1986, EPA report /600/S3-89/058, 1989.

Shields, H.C., Weschler, C.W., and Naik, D.: Ozone removal by charcoal filters after continuous extensive use (5 to 8 years), Proceedings of the 8th International Conference on Indoor Air Quality and 805   Climate, Indoor Air 99, Edinburgh, Scotland, Aug. 8-13, Vol. 4, 49-54, 1999.

Smith, D.M. and Chughtai, A.R.: Reaction Kinetics of Ozone at Low Concentrations with n-Hexane Soot, J. Geophys. Res., 101, 19607-19620, 1996.

810   Spicer, C.W., Joseph, D.W., and Ollison, W.M.: A re-examination of ambient air ozone monitor interferences, J. Air Waste Manage. Assoc., 60:11, 1353-1364, doi:10.3155/1047-3289.60.11.1353, 2010.

Stephens, S.L., Birks, J.W. and Calvert, J.G.: Ozone as a Sink for Atmospheric Carbon Aerosols Today and Following Nuclear War, Aerosol Sci. Technol. 10, 326-331, 1989.
815

Tracz, A., Wegner, G., and Rabe, J.P.: Scanning tunneling microscopy study of graphite oxidation in ozone-air mixtures, Langmuir, 19, 6807-6812, 2003.

U.S.-EPA, Laboratory Study to Explore Potential Interferences to Air Quality Monitors, EPA-454/C-00-820   002, Office of Air Quality Planning and Standards: Research Triangle Park, NC, 1999.

U.S.-EPA, https://www.epa.gov/ozone-pollution-and-your-patients-health/health-effects-ozone-general-population, visited 10/2016.

825   Weisel, C.P., Cody, R.P., and Lioy, P.J.: Relationship between summertime ambient ozone levels and emergency department visits for asthma in central New Jersey, Environ. Health Perspect., 103 (suppl. 2), 97-102, 1995.

Weiss-Penzias, P., Jaffe, D.A., McClintick, A., Prestbo, E., and Landis, M.S.: Gaseous elemental 830   mercury in the marine boundary layer: Evidence for rapid removal in anthropogenic pollution, Environ. Sci. Technol., 37, 3755-3763, 2003.

White, M.C., Etzel, R.A., Wilcox, W.D., and Lloyd, C.: Exacerbations of childhood asthma and ozone pollution in Atlanta, Environ. Res., 65, 56-68, 1994.

835

Wilson, K.L., and Birks, J.W.: Mechanism and elimination of a water vapor interference in the measurement of ozone by UV absorbance, Environ. Sci. Technol., 40, 6361-6367, 2006.

Zdanevitch, I.: Study of Ozone Measurement Interferences: Final Report, DRC-02-39246-AIRE-673-v2-Izd; Institut National de L'Environnement Industriel et des Risques (INERIS): Verneuil-en-Halatte, France, 2002.

840

Table 1. Properties of VOCs and other atmospheric species that are potential interferents in UV
absorption-based ozone measurements.

Interferent (INT)	Ambient mixing ratio[a], ppb	σ_{254},[b] 10^{-17} cm^2 molecule^{-1}	e_v,[c] (25°C) mm Hg	S,[d] ppb INT/ppb O$_3$
Used in this Study				
p-Xylene	0.3 – 30	0.057	8.84	20.2
Phenol	≤ 0.02	0.16	0.350	7.1
p-Tolualdehyde	< 1	0.55	0.250	2.09
o-Nitrophenol	≤ 0.001	2.15	0.113	0.53
Mercury	0.0002-0.003	1860[d]	0.002	0.0005
Typical Atmospheric Constituents				
NO$_2$	≤ 100	0.001	741	1000
SO$_2$	1 -25	0.014	3000	77
Methanol	≤ 40	< 0.00001	127	> 10000
Acetone	0.2 - 9	0.0030	231	290
Formaldehyde	0.5 – 75	0.00029	3890	3960
Acetaldehyde	0.1 – 18	0.0015	902	590
1,3-Butadiene	0.1 – 6	< 0.02	1840	> 58
Trichloroethene (TCE)	≤ 0.2	0.0041	69	265
2-Butanone	0.1 – 8	0.0031	90.6	370
Isoprene	0.1 – 5.5	0.0052	550	220
Octane	0.02 - 13	< 0.0002	14.1	> 5700
Methacrolein	0.02 – 1.7	0.00018	155	6400
Methyl Vinyl Ketone	0.2 – 1.5	0.00024	152	4790
Acetic Acid	0.5 – 10	< 0.0006	15.7	> 1900
α-Pinene	≤ 0.4	0.00054	4.75	2120
d-Limonene	≤ 0.1	0.015	1.55	77
Aromatics				
Benzene	0.9 – 26	0.03	94.8	38
Toluene	0.05 – 39	0.039	28.4	29
o-Xylene	0.4 – 1	0.048	6.5	24
Ethyl Benzene	0.08 – 16.5	0.052	9.6	22
Styrene (vinyl benzene)	0.06 – 3.1	1.3	6.4	0.88
1,3,5-Trimethylbenzene	0.03 – 4.2	0.037	2.48	31
m-Cresol	≤ 0.004	0.108	0.11	10.6
Benzaldehyde	0.1 – 1	0.09	0.127	12.8
Naphthalene	0.01 – 0.1	1.07	0.08	1.07
Nitrobenzene	0.02-0.40	1.3	0.245	0.88

a. Typical concentration ranges reported in Finlayson-Pitts and Pitts (2000); Seila et al. (1989); Mahmoud et al., (2002); Bernardo-Bricker et al., (1995); Delhomme et al., (2010); Davies, L. (2003); Eiguren-Fernandez et al. (2004); Liu et al (2002); Denis et al, (2006).
b. Absorbance cross sections at 253.7 nm taken from the Keller-Rudek et al., 2013 and related web data base (*http://www.uv-vis-spectral-atlas-mainz.org/*)
c. Vapor pressures taken from *http://pubchem.ncbi.nlm.nih.gov/*.
d. Selectivity ratio, $S = \sigma_{O_3} / \sigma_{int}$ at 253.7 nm. To estimate the maximum response that a particular interferent could give in an ozone monitor, divide the Ambient Mixing Ratio by the Selectivity ratio, S.
e. From Birks et al. (2009).

Table 2. Summary of results from tests of VOC interferences in dry air.

Volatile Organic Compound	Scrubber	Slope, ppb O_3/ppb VOC	S^a, ppb VOC / ppb O_3	S, Previous Results
p-xylene	2B Hopcalite	0.056 ± 0.004	17.9	
	Thermo Electron (MnO_2)	0.051 ± 0.003	19.6	
	Teledyne-API (MnO_2.)	0.046 ± 0.005	21.7	
	Heated Graphite	0.012 ± 0.001	83.3	
phenol	2B Hopcalite	0.21 ± 0.01	4.76	
	Thermo Electron (MnO_2)	0.18 ± 0.01	5.56	$7.7\text{-}14.3^b$
	Teledyne-API (MnO_2)	0.20 ± 0.01	5.00	
	Heated Graphite	0.051 ± 0.004	19.6	
p-tolualdehyde	2B Hopcalite	1.71 ± 0.25	0.58	$0.0\text{-}2.0^c$
	Thermo Electron (MnO_2)	1.57 ± 0.43	0.63	1.25^c
	Teledyne-API (MnO_2)	1.54 ± 0.10	0.65	
	Heated Graphite	0.08 ± 0.02	12.5	
		0.28 ± 0.06^d	3.6	
o-nitrophenol	2B Hopcalite	7.7 ± 0.5	0.13	$0.55\text{-}0.91^c$
	Thermo Electron (MnO_2)	8.0 ± 0.3	0.13	0.45^c
	Teledyne-API (MnO_2)	7.4 ± 0.3	0.14	
	Heated Graphite	1.1 ± 0.3	0.91	
		2.7 ± 0.2^d	0.37	

860   a.   S = 1/Slope, measured Selectivity Ratio.
b.   Zdanevitch, 2002.
c.   Spicer et al., 2010.
d.   Results from 2 different sets of graphite tubes.

865
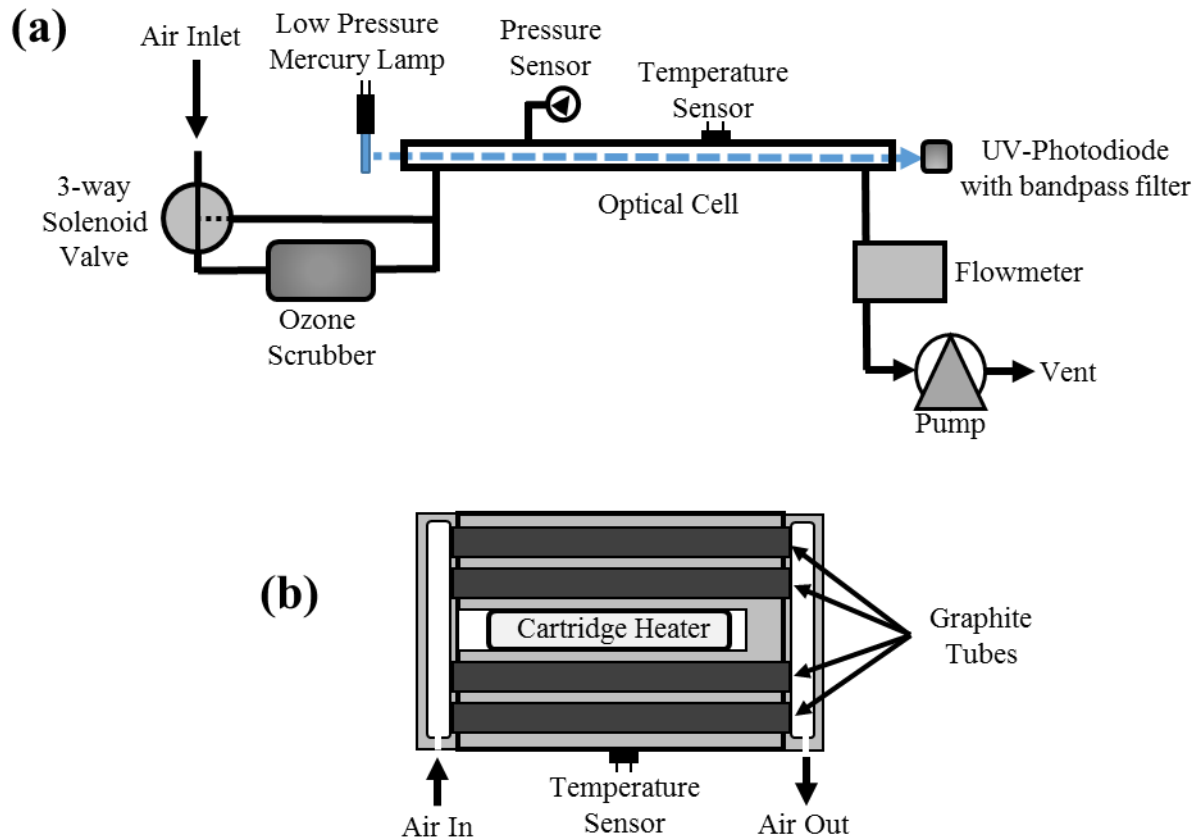
Figure 1. (a) Schematic diagram of a typical single-beam UV absorbance monitor for ozone. (b) Schematic of the heated graphite scrubber consisting of four graphite tubes contained within a temperature-controlled aluminum block.
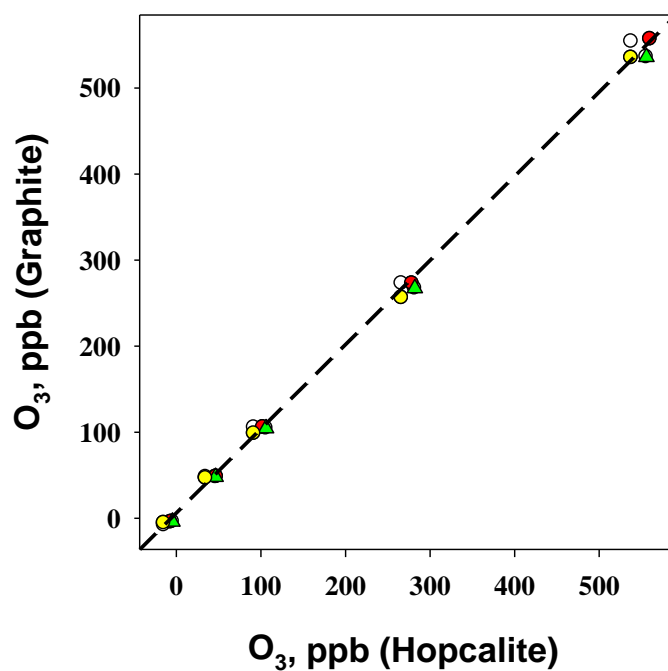
Figure 2. Plot of ozone measured with the graphite scrubber (at 100°C) vs. that measured with the conventional Hopcalite scrubber. The different symbols/colors represent different sets of graphite tubes used within the heater during our reproducibility testing. Results were obtained using a 2B Technologies Model 202 single-beam ozone analyzer. The dashed line drawn is the 1:1 line.

875
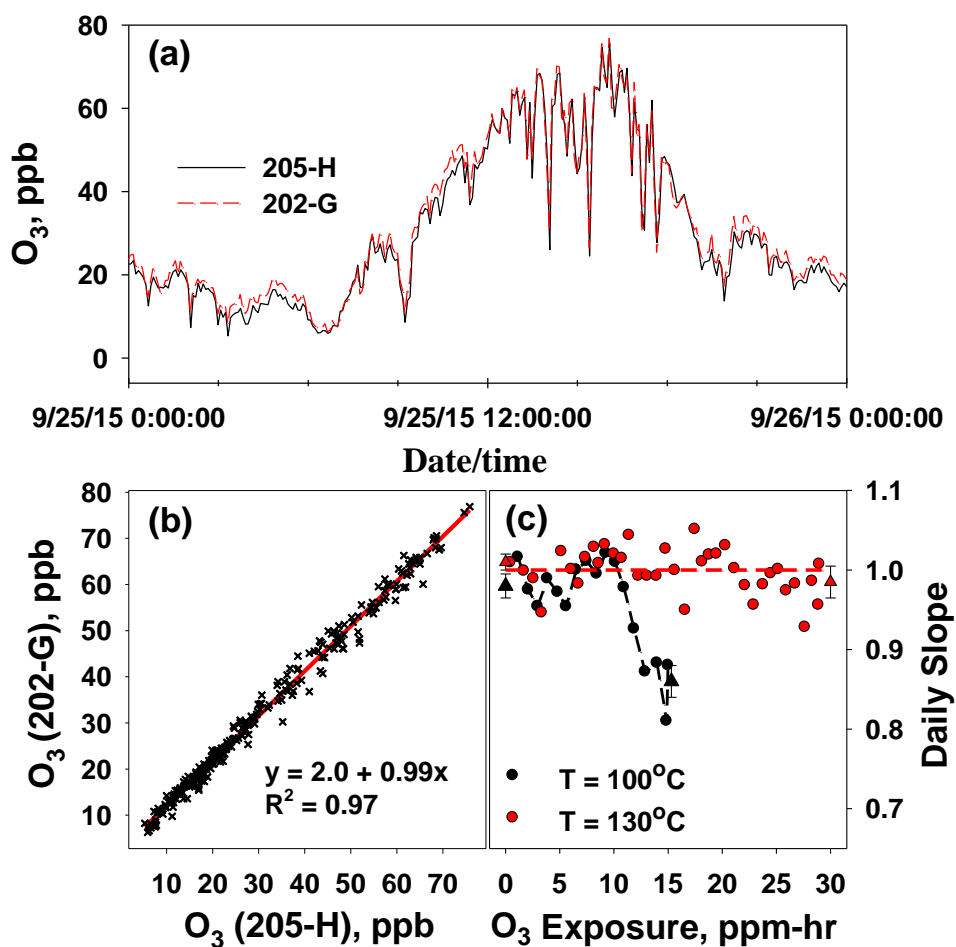
Figure 3. (a) Time series of 5-min averaged ozone concentrations measured in Boulder, CO on September 26, 2015. (b) Correlation plot between the Model 202 (202-G, equipped with graphite scrubber) and the FEM Model 205 (205-H, Hopcalite scrubber and Nafion) for September 26, 2015. (c) Plot of the daily correlation plot slope vs. cumulative ozone exposure for the 202-G analyzer. Each point represents a single day. The graphite scrubber was initially maintained at 100°C, regenerated, and then operated at 130°C (see text for further explanation). Triangles represent calibration slopes pre- and post-intercomparison.
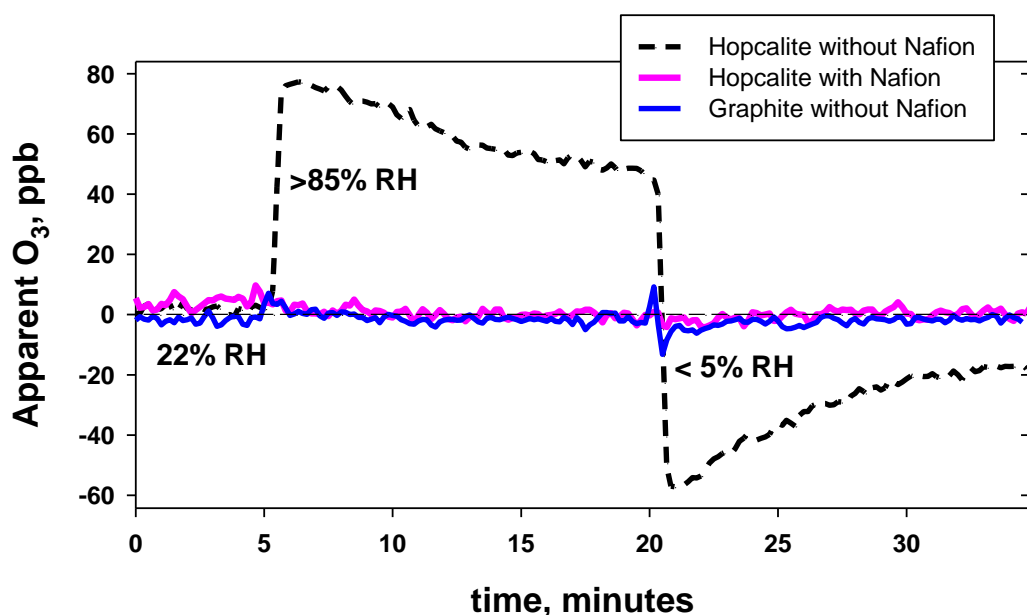
Figure 4. Time series showing the response of a Model 202 ozone analyzer to changes in relative humidity with no ozone present and different scrubbers.

890
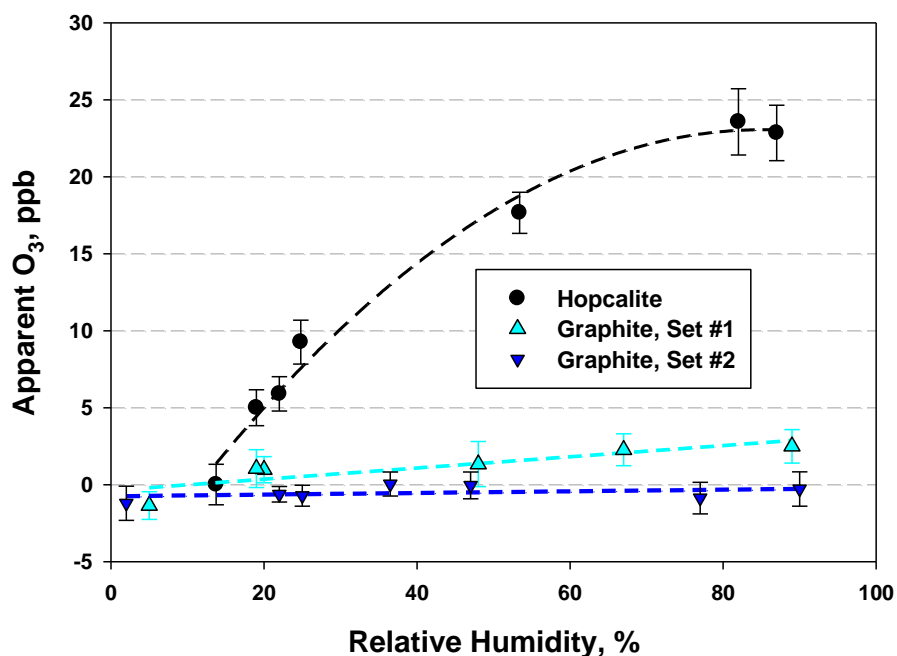
Figure 5. Humidity dependence of two different heated (100°C) graphite scrubbers as well as that of a Hopcalite scrubber. The ozone analyzer was 2B Technologies Model 202 single-beam instrument. Data points were 2-minute averages obtained 15 minutes after a change in relative humidity. Error bars are 1σ of the 2-minute average. The experiment was conducted at 20°C. Note that the step changes in humidity
895 were not as large as those shown in Figure 4, thus leading to smaller observed artefact signals for the Hopcalite scrubber.
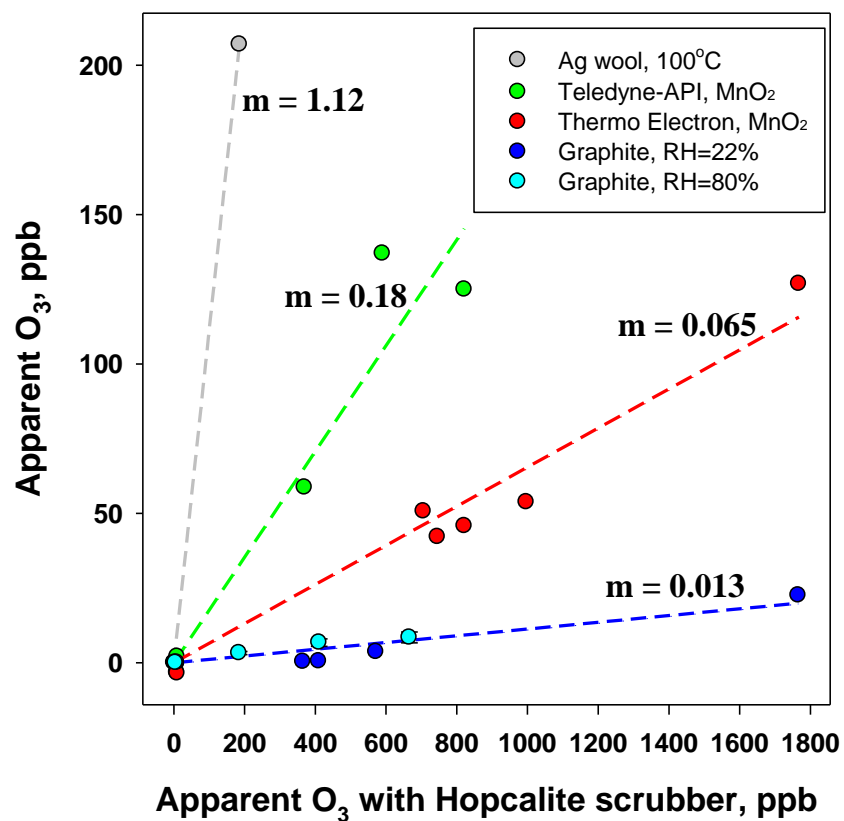
Figure 6. Apparent ozone measured in the Model 202 single-beam ozone analyzer using different ozone scrubbers, relative to the standard Hopcalite scrubber, upon addition of mercury vapor to ozone-free air. Slopes are given by the m-values. The graphite scrubbers were heated to 100°C for these tests.

900

905
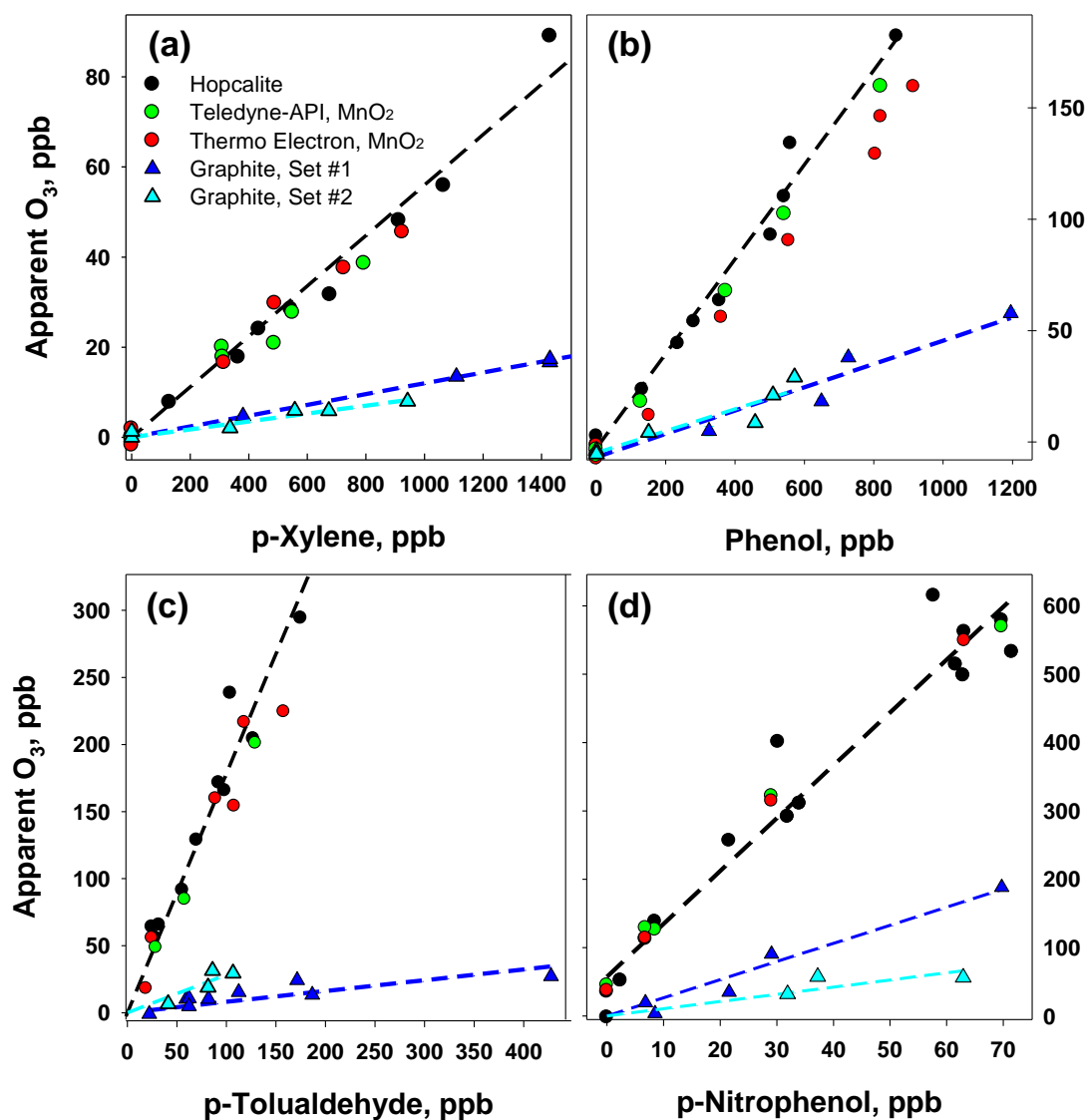
Figure 7. Apparent ozone vs. VOC concentration in dry, ozone-free air for different scrubber types and four different VOCs of varying absorption cross section at 253.7 nm. Data from two different sets of graphite tubes are shown (Set #1 and Set #2). Slopes are given in Table 2.

910
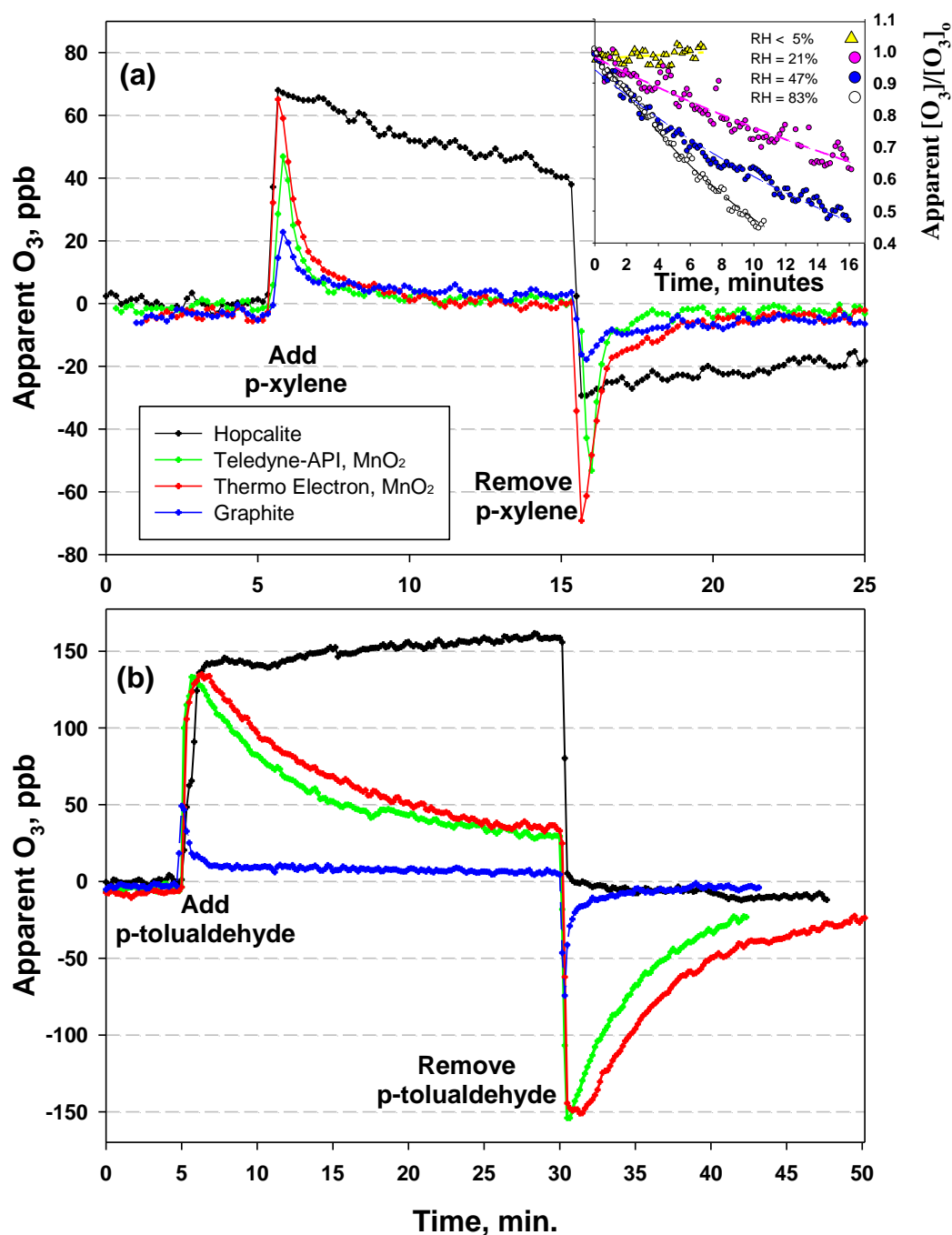
Figure 8. (a) Plot of the temporal behavior of the apparent ozone at 38% RH as 1.2 ppm of p-xylene is added (t = 5 min) and then removed (t = 15 min) from ozone-free air for various scrubbers. Inset: Temporal decay of the fractional apparent ozone ($[O_3]_o$ = initial concentration) as a function of relative humidity upon addition of ~ 1.3 ppm of p-xylene to a Model 202 analyzer equipped with a packed-bed 915 Hopcalite scrubber. (b) Temporal behavior of the apparent ozone at 75% RH as ~ 90 ppb of p-tolualdehyde was added (t = 5 min) and then removed (t = 30 min) for various scrubbers.

920
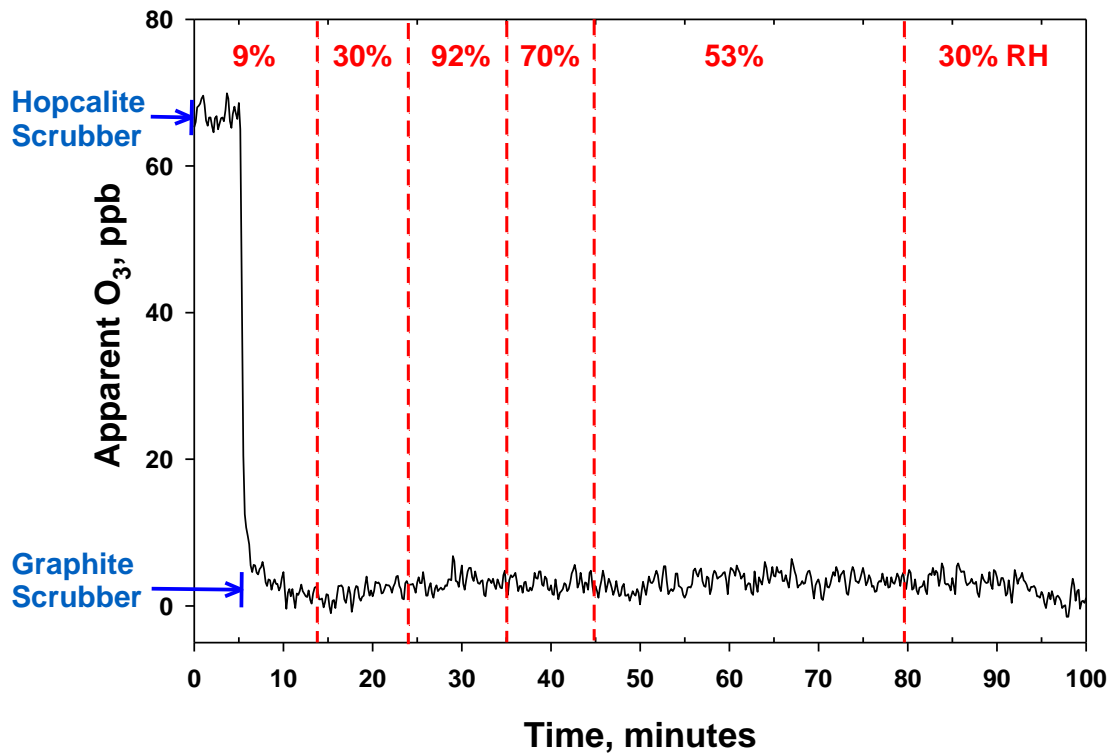
Figure 9. Apparent ozone observed upon addition of ~1.3 ppm of p-xylene to ozone-free air. Initially, the ozone analyzer was equipped with the standard Hopcalite scrubber (Apparent O_3 concentration= 67 ppb). The Hopcalite was replaced with the heated graphite scrubber at time = 5 minutes. Over the next 925 95 minutes, the relative humidity of the air was varied as designated by the red vertical dashed lines.